

Analysis of Compressible Diblock Copolymer Melts That Microphase Separate upon Cooling

Junhan Cho

Department of Polymer Science and Engineering, and Hyperstructured Organic Materials Research Center, Dankook University, San-8, Hannam-dong, Yongsan-gu, Seoul 140-714, Korea

Received January 18, 2001; Revised Manuscript Received May 7, 2001

ABSTRACT: A Landau mean-field analysis is performed to study microphase separation upon cooling in a compressible diblock copolymer with the identical compressibility for both blocks. The inhomogeneity of free volume as well as that of the density of each block is analyzed in the weakly microphase separated system. Excess free volume is shown to be located at the interface between microphase domains in order to screen unfavorable energetics between dissimilar blocks. The phase diagram determined for the copolymer is shown to be closely related to that of the incompressible counterpart. In particular, a symmetric copolymer with no compressibility difference between blocks is found to exhibit a critical point. It is revealed that the relevant parameters for the phase behavior of the copolymer are composition and $r_1\chi_{\text{app}}$, where r_1 is the chain size and χ_{app} an apparent Flory–Huggins interaction parameter that is dependent not only on temperature but also on compressibility. A model-specific form of χ_{app} is suggested here to describe in a unified way the effects of temperature, pressure, and chain size on the phase diagram.

1. Introduction

Block copolymers from chemically binding two or more different homopolymers have drawn much attention from polymer society. Various microscopically ordered structures, called microphases, are formed owing to their nanoscale self-assembly behavior. Block copolymers, therefore, lead to diversified applications as thermoplastic elastomers, compatibilizers, surface modifiers, and photoresists.^{1–4}

Block copolymers from incompatible polymers exhibit a microphase separation from a disordered state to an ordered state upon cooling, which is called the upper critical ordering transition (UCOT) behavior. The UCOT behavior is driven by the unfavorable interactions between polymers comprising a given block copolymer. Ordered morphologies formed after microphase separation are divided into classical and complex morphologies. The former includes body-centered cubic spheres (bcc), hexagonally packed cylinders (hex), and lamellar (lam) structures. Recently found morphologies such as bicontinuous gyroid and hexagonally perforated lamellar structures are categorized as the latter.^{3,4}

In recent decades, extensive theoretical works have been performed to analyze equilibrium microstructures of block copolymers in a molten state or in solution and transitions between them.⁴ In particular, Leibler applied a Landau mean-field analysis based on the random-phase approximation (RPA) to weakly segregating diblock copolymer melts near spinodals.⁵ A general sequence of transitions from a disordered state to a metastable bcc, then to a hex, and then finally to a lam morphology upon cooling was established for asymmetric diblock copolymers. A symmetric one was shown to possess a critical point, where the copolymer shows a continuous transition from the disordered state to the lam morphology without evoking any metastable state. Leibler's mean-field theory was later corrected by Fredrickson and Helfand to include fluctuation effects.⁶ It was shown that for a copolymer of finite molecular weight no critical point exists and the direct transition to the hex or lam morphology is possible. While those theories deal only with the classical morphologies, more advanced block copolymer theories have emerged in order to analyze

complex morphologies.⁴ Harmonic corrections to the Leibler and Fredrickson–Helfand theories have been suggested by Milner and Ohlmsted⁷ and by Hamley and Podnek^{8–11} to interpret the gyroid as a stable microphase between the hex and the lam morphologies.

All of the theories for block copolymers just mentioned^{4–11} are based on the common assumption of system incompressibility. Russell et al. recently found some diblock copolymer melts exhibiting microphase separation upon heating, which is also referred to as lower critical ordering transition (LCOT).^{12–15} There has since been a definite need for finite compressibility because such thermally induced microphase separation is driven by the differences in volume fluctuations between constituent polymers. To interpret the LCOT behavior, especially radiation scattering or spinodals from LCOT systems, efforts to introduce finite compressibility into RPA have been exerted by several research groups. Freed and co-workers were the first to incorporate finite compressibility into the incompressible RPA by allowing for vacancy.^{16–23} Other theories have also been formulated using vacancies as a pseudosolvent in the incompressible treatment.^{24–26}

Recently, a new compressible RPA theory was introduced by the present author.^{27,28} The theory is unique in the sense that the pseudosolvent technique was not employed in formulating the theory. Akcasu's general compressible RPA formalism,^{29,30} which discards the Lagrange multiplier for the incompressibility constraint in RPA calculations, was used instead. Finite compressibility was incorporated into the theory through effective RPA interaction fields stemming from an off-lattice equation-of-state (EOS) model in Appendix A, which was developed by Cho and Sanchez (CS).³¹ The vertex functions in the Landau expansion of the free energy in packing density fluctuations for diblock copolymer melts were formulated up to quartic order.²⁸ A Landau free energy density was then derived for the classical morphologies of LCOT diblock copolymer melts. It was shown from the Landau analysis that a general sequence of microphase transition upon heating (disorder \rightarrow bcc \rightarrow hex \rightarrow lam) is observed for LCOT systems. However, it was revealed that LCOT systems do not

possess a critical point. It was also shown that the inhomogeneity of free volume is induced by microphase separation. Excess free volume is found to be present in the domains rich in the more compressible constituent.

It is the objective of our study here to derive a Landau free energy density based on the CS model for typical, but compressible UCOT diblock copolymer melts. The unfavorable cross association between constituent polymers leads to the self-assembly behavior. As the simplest but the most important case, compressibility difference between constituents is assumed to be absent, although each constituent is compressible. A leading harmonic is solely employed to describe a given morphology, so that only classical morphologies are considered in this study. Hence, the present theory can be regarded as a primary generalization of Leibler's theory for the incompressible cousins to include compressibility effects. Microphase separation may also induce the inhomogeneity of free volume in the UCOT systems. Unlike LCOT systems, however, excess free volume is expected to be present at the interface between domains to screen unfavorable cross interactions.³² Such an intuitive idea yields a reasonable treatment of the packing density and free volume fluctuations. This procedure then results in the desired analytical Landau free energy density for the copolymers. It is shown from the formulated Landau free energy that compressible UCOT systems, with identical compressibilities for both constituents, possess a critical point. The relevant parameters for determining the phase behavior of these compressible systems are extracted from the theory.

The present theory, based on the mean-field approach, possesses the same limitations as Leibler's. Chains in a given system are assumed to be ideal. Therefore, chain-stretching effects are not considered. Concentration fluctuation effects are also ignored in this mean-field calculation. Improvement in the present theory by correcting its limitations along with employing multiple harmonics is expected to give substantial changes in the mean-field phase diagram such as the vanishing continuous transition. Such a sophisticated treatment may be the subject of our future study. The principal merit of the present study on UCOT systems, though based on the mean-field approximation, is its capability to probe pressure effects on microphase separation transition and subsequent transitions between ordered microstructures. Such pressure-induced microphase separation is indeed important in designing and controlling self-assembled microstructures because normal processing conditions always involve the exertion of pressure.

A diblock copolymer of polystyrene (PS) and polybutadiene (PBD), denoted as P(S-*b*-BD), is a typical example of a UCOT system. We, therefore, choose this copolymer as a model system. The present Landau analysis is used to calculate the phase behavior of the copolymer, especially changes caused by applying pressure. Stamm and co-workers measured the order-disorder transition temperature of a symmetric P(S-*b*-BD) melt with varying pressure using small-angle X-ray scattering techniques.³³ The experimental results for the copolymer are to be compared with our theory.

II. Theory

Consider a system of A-B diblock copolymers with r_i monomers of the i th component, where $i = 1$ and 2 correspond to A and B, respectively, to have the overall

size $r_T (= \sum_i r_i)$. The system is allowed to be compressible: there is free volume in the system. We denote as η_i the global packing density of i -monomers that implies the fraction of system volume occupied by all the monomers of the i th component. Then $\eta_i(\vec{r})$ represents the local packing density of such monomers at a position \vec{r} . Phase segregation in the system can be probed by considering the average packing density fluctuations, or the order parameter ψ_i for the i -monomers. The order parameter ψ_i is defined as

$$\psi_i(\vec{r}) \equiv \langle \delta \eta_i(\vec{r}) \rangle = \langle \eta_i(\vec{r}) - \eta_i \rangle \quad (1)$$

where the brackets in eq 1 imply the thermal average. In a Landau mean-field approach, the free energy for the system can be expanded as a series in the order parameter ψ_i as

$$F - F_0 = \frac{1}{\beta n} \sum_{n=2}^{\infty} \frac{1}{n!} \int d\vec{q}_1 \dots d\vec{q}_n \Gamma_{i_1 \dots i_n}^{(n)}(\vec{q}_1, \dots, \vec{q}_n) \psi_{i_1}(\vec{q}_1) \dots \psi_{i_n}(\vec{q}_n) \quad (2)$$

where the F_0 implies the free energy in a disordered state and $\beta = 1/kT$ has its usual meaning. In the above equation, the Fourier component of ψ_i has been used for the convenience of subsequent manipulation of the free energy. The \vec{q}_i in eq 2 denotes physically the scattering vector as phase segregation is often investigated by radiation scattering techniques. The coefficient $\Gamma_{i_1 \dots i_n}^{(n)}$ is commonly known as the n th-order vertex function. Such vertex functions based on the compressible RPA in connection with the CS model are explicitly written in Appendix B.

For the analysis of compressible UCOT diblock copolymer systems, we perform a simple transformation of the order parameters in eq 1 into the following ones.³⁴

$$\bar{\psi}_1 \equiv \frac{1}{\eta} [(1 - \phi_1)\psi_1 - \phi_1\psi_2] \quad (3)$$

$$\bar{\psi}_2 \equiv \psi_1 + \psi_2 \quad (4)$$

where $\phi_1 \equiv r_1/r_T$ defines the close-packed volume fraction of A monomers on copolymer chains. The ϕ_2 then indicates the volume fraction of B monomers and thus $\phi_2 = 1 - \phi_1$. In eq 3, η denotes the total packing density satisfying $\eta = \eta_1 + \eta_2$. The η_i is indeed equated to $\phi_i \eta$. It is easily seen that $\eta_1 + \eta_2 = 1 - \eta_f$, where η_f implies the fraction of free volume in the system. The $-\bar{\psi}_2$ is then rendered to the average fluctuations in free volume fraction, $\langle \delta \eta_f \rangle$, because $\psi_1 + \psi_2 = -\langle \delta \eta_f \rangle$. The inhomogeneity of the free volume is, therefore, probed through $\bar{\psi}_2$. These new order parameters are convenient in the case of UCOT systems. It can be said that $\bar{\psi}_2$ goes to zero as free volume is completely squeezed out. In such a case, $\bar{\psi}_1$ becomes the only order parameter left, to be equal to simply ψ_1 . The compressible RPA then converges to the incompressible case so that a direct comparison of the present analysis with that by Leibler⁵ is possible. The vertex functions can be redefined in accord with the new order parameters as

$$\Gamma_{i_1 \dots i_n}^{(n)}(\vec{q}_1, \dots, \vec{q}_n) \psi_{i_1}(\vec{q}_1) \dots \psi_{i_n}(\vec{q}_n) = \bar{\Gamma}_{i_1 \dots i_n}^{(n)}(\vec{q}_1, \dots, \vec{q}_n) \bar{\psi}_{i_1}(\vec{q}_1) \dots \bar{\psi}_{i_n}(\vec{q}_n) \quad (5)$$

In Appendix C, the explicit mathematical expressions

are given for the new vertex functions. It should be perceived that both $\Gamma^{(n)}$ and $\bar{\Gamma}^{(n)}$ are vanishing unless $\sum_{i=1}^n \bar{q}_i = 0$.

As microphase segregation develops, each component of the copolymer fluctuates in its concentration. The ordered pattern is simply described as the superposition of plane waves or harmonics. The free energy expansion in eq 2 is approximated to the sum containing only the most important contributions from the fastest growing waves with wavelength q^* .⁵ The observed ordered structures are then represented by a set of n wave vectors \bar{Q}_i 's ($i = 1, \dots, n$), whose lengths are all q^* . There need six and three wave vectors for bcc and hex morphologies, respectively, and one wave vector for lam morphology. Those wave vectors are tabulated elsewhere.⁵ Free volume possesses no preference for a particular block because there is no compressibility difference between blocks. Therefore, free volume acts as a neutral solvent. We intuitively expect that the excess free volume is present at the interface between two incompatible polymers in order to screen the unfavorable interactions. The fraction of free volume then fluctuates with the wavenumber $2|\bar{Q}_i|$. The order parameters to describe a given microphase morphology can, therefore, be parametrized as

$$\bar{\psi}_1(\vec{r}) = 2 \frac{1}{\sqrt{n}} \bar{\psi}_n(1) \sum_{k=1}^n \cos[\bar{Q}_k \cdot \vec{r} - \varphi_k(1)] \quad (6)$$

$$\bar{\psi}_2(\vec{r}) = 2 \frac{1}{\sqrt{n}} \bar{\psi}_n(2) \sum_{k=1}^n \cos[2\bar{Q}_k \cdot \vec{r} - \varphi_k(2)] \quad (7)$$

where $\bar{\psi}_n(i)/\sqrt{n}$ and $\varphi_n(i)$ indicate the amplitude and the phase angle, respectively, for the order parameter $\bar{\psi}_i(\vec{r})$.

After the consideration of phase angles to minimize the Landau free energy, it can be shown that the free energy is reduced to

$$\delta\beta F = \beta(F - F_0) = \bar{\Gamma}_{11}^{(2)}(q^*) \bar{\psi}_n(1)^2 - \frac{\eta a_n}{r_T} \bar{\psi}_n(1)^3 + \frac{\eta b_n}{r_T} \bar{\psi}_n(1)^4 + \bar{\Gamma}_{22}^{(2)}(2q^*) \bar{\psi}_n(2)^2 + \frac{1}{3} \Pi \bar{\psi}_n(1)^2 \bar{\psi}_n(2) \quad (8)$$

where a_n and b_n are identical with α_n and β_n (eqs V-10, 11, 14, 15, and 26 in ref 5) for a proper microphase morphology, respectively, in the Landau free energy by Leibler for incompressible UCOT diblock copolymer melts. Those values thus represent the uncoupled higher-order vertex functions. It is noted that there is no coupled quadratic term, $\bar{\Gamma}_{12}^{(2)}$, because \bar{Q}_i and $-2\bar{Q}_i$ do not cancel out. It is perceived that $\bar{\psi}_n(2)$ representing the free volume inhomogeneity is far smaller than $\bar{\psi}_n(1)$ for the inhomogeneity of each component density. The Π then collects the lowest-order coupled vertex functions as

$$\Pi = \frac{c_n}{2} \frac{1}{(\sqrt{n})^3} \{ \bar{\Gamma}_{112}^{(3)} + \bar{\Gamma}_{121}^{(3)} + \bar{\Gamma}_{211}^{(3)} \} \quad (9)$$

where c_n is equal to 12, 6, and 2 for bcc ($n = 6$), hex ($n = 3$), and lam ($n = 1$) morphologies, respectively. It should be noted that those three terms in eq 9 are nonvanishing coupled ones involving two \bar{Q}_i 's and one

Table 1. Various Molecular Parameters for Homopolymers Used in This Study

polymer	σ_i (Å)	$\bar{\epsilon}/k$ (K)	$r_i \pi \sigma_i^3 / 6MW_i^a$ (cm ³ /g)
PS ^b	4.039	4107.0	0.418 57
PBD ^c	4.040	4065.9	0.493 95

^a This combined parameter represents the close-packed molecular volume of a given polymer with the molecular weight MW. To obtain the chain size r_i , MW should be given. ^b Volume data are obtained from ref 35. The average error between experimental and calculated volume is 0.000 69 cm³/g. ^c Volume data are obtained from ref 36. The σ is fixed while fitting volume data to eq A3. The average error reaches 0.001 58 cm³/g. The accuracy of the theoretical equation of state in correlating the volume data can be enhanced by taking σ as one of molecular parameters to be fitted.³¹

$-2\bar{Q}_i$ to sum up to none. The remaining terms involving in $\bar{\psi}_n(2)^3$, $\bar{\psi}_n(2)^4$, and $\bar{\psi}_n(1)^2 \bar{\psi}_n(2)^2$ are ignored because such higher-order terms would add trivial contributions to the free energy. Equation 8 can be further manipulated to yield the following condition for $\bar{\psi}_n(2)$ to minimize the free energy:

$$\bar{\psi}_n(2) = -\frac{1}{6} \frac{\Pi}{\bar{\Gamma}_{22}^{(2)}(2q^*)} \bar{\psi}_n(1)^2 \quad (10)$$

Equation 10 shows that $\bar{\psi}_n(2)$ is of the order $\bar{\psi}_n(1)^2$. The $\bar{\psi}_n(2)$ is thus quite small as expected, because $\bar{\psi}_n(1) \ll 1$. Putting eq 10 into eq 8 gives the final expression for the desired Landau free energy to analyze microphase equilibria as

$$\delta\beta F = \bar{\Gamma}_{11}^{(2)}(q^*) \bar{\psi}_n(1)^2 - \frac{\eta a_n}{r_T} \bar{\psi}_n(1)^3 + \left[\frac{\eta b_n}{r_T} - \frac{1}{36} \frac{\Pi^2}{\bar{\Gamma}_{22}^{(2)}(2q^*)} \right] \bar{\psi}_n(1)^4 \quad (11)$$

The order-disorder and order-order transitions are now to be determined by the minimization of eq 11 with respect to the only remaining $\bar{\psi}_n(1)$. It can be shown that the Π in the second part of the quartic term is proportional to $1/r_T^2$. Therefore, the term with Π^2 is overwhelmed by $\eta b_n/r_T$, if the chain size is big enough.

III. Calculation of Phase Diagrams

The formulated Landau free energy is now applied to a typical UCOT diblock copolymer system to determine transition temperatures. It was already mentioned in the Introduction that P(S-*b*-BD) is chosen here as a model system. To characterize the P(S-*b*-BD) system, one needs various molecular parameters based on the CS model in Appendix A. Those parameters include the self-interaction parameter $\bar{\epsilon}_{ii}$, the monomer diameter σ_i , and the chain size r_i for pure polymers and the parameter $\bar{\epsilon}_{ij}$ for cross interaction between different polymers.

In Table 1, the molecular parameters for the two constituents, PS and PBD, are tabulated. The parameters just given have been used in our previous work on introducing the present RPA theory.²⁷ It is seen in this table that a combined parameter, $r_i \pi \sigma_i^3 / 6MW_i$, where MW is the molecular weight of a given constituent polymer, is presented instead of the chain size r_i . r_i can be obtained from setting proper molecular weights. Subscripts 1 and 2 hereafter indicate PS and PBD, respectively. The parameters for PS were determined by fitting volume data of PS measured by Quach and Simha³⁵ to the equation of state in eq A3 from the CS

model. In the case of PBD, the parameters were obtained from fitting its volume data given by Barlow³⁶ to eq A3, adjusting only $\bar{\epsilon}_{22}$ and r_2 with a fixed σ_{22} ($=\sigma_{11}$).³⁷ As far as representing the volume data of pure PBD is concerned, such two-parameter fitting does not offer the best set of parameters. It is seen that the fitted $\bar{\epsilon}_{22}$ of PBD is similar to that of PS. This result implies that the interaction strength for PBD per a volume unit ($\sim\sigma_{11}^3$) is similar to that for PS. The compressibility difference between PS and PBD is thus suppressed. However, as was shown in our previous communication, the cross-interaction parameter $\bar{\epsilon}_{12}$ of 0.99565 ($\bar{\epsilon}_{11}\bar{\epsilon}_{22}$)^{1/2} together with the homopolymer parameters in Table 1 yields rather an accurate estimation of cloud points for the PS/PBD blends of low molecular weights.²⁷ This observation suggests that compressibility difference between the two homopolymers is not an important factor in describing the phase behavior of these blends. The chosen $\bar{\epsilon}_{12}$ yields $[\bar{\epsilon}_{11} + \bar{\epsilon}_{22} - 2\bar{\epsilon}_{12}]/2k = 17.828$ K, which represents the unfavorable energetics as the driving force of the observed phase separation in the PS/PBD system.³⁸ This $\bar{\epsilon}_{12}$ is used in the following calculations for the corresponding block copolymers. The P(S-*b*-BD) system with their molecular parameters indeed suits our purpose to investigate a compressible UCOT system exhibiting no compressibility difference between constituents.

Transition temperatures including spinodals can now be obtained from eq 11. The spinodals are typically determined by the vanishing linear term of the Landau free energy, which is $\bar{\Gamma}_{11}$ here. Equation C4 shows $\bar{\Gamma}_{11} = \eta^2(\Gamma_{11} - 2\Gamma_{12} + \Gamma_{22})$, which then yields $\Gamma_{12} = (\Gamma_{11} + \Gamma_{22})/2$, i.e., arithmetic mean, at spinodals. From our previous communication,^{27,28} it was shown that the exact spinodals are given by the vanishing determinant, $\det[\Gamma_{ij}] = 0$, which implies $\Gamma_{12} = \sqrt{\Gamma_{11}\Gamma_{22}}$, i.e., the geometric mean. In the present calculation, there is little difference between the two spinodals given above. Such a result is caused by the fact that $\bar{\epsilon}_{22}$ employed here is close to $\bar{\epsilon}_{11}$. The Γ_{ij} is approximated in the compressible RPA to the combination of the correlation function S_{ij}^0 for noninteracting Gaussian chains and the interaction field W_{ij} as $\Gamma_{ij} = S_{ij}^{0-1} + \beta W_{ij}$. The interaction field W_{ij} , formulated from the CS model, is presented explicitly in eqs B4–B6. As W_{ij} describes the effective interaction (energetic + entropic) between two nonbonded monomers, the W_{ij} for a long chain system becomes independent of the chain size r_T . The chains then experience $|S_{ij}^{0-1}| \ll |\beta W_{ij}|$ because S_{ij}^{0-1} scales as $1/r_T$. The W_{ij} is shown to be dominantly affected by $\bar{\epsilon}_{ij}$, as can be seen from eq B6. Therefore, it is observed that $\Gamma_{11} \approx \Gamma_{22}$ in the case that $\bar{\epsilon}_{11} \approx \bar{\epsilon}_{22}$. To illustrate this point, Γ_{11} and Γ_{22} along with the corresponding S_{ij}^{0-1} 's at ambient pressure and at spinodal temperatures are tabulated against composition in Table 2. It is common sense that there is little difference between spinodals from arithmetic and geometric means in this case.

The cubic order term in eq 11 is identical to that in Leibler's Landau free energy in the incompressible situation except the packing density η . Therefore, the cubic term vanishes at $\phi_{PS} = 0.5$, which yields a continuous second order transition and a critical point. This observation extends a commonly believed notion on the continuous transition as a characteristic of incompressible UCOT systems to a more general situation; the continuous transition is also characteristic of

Table 2. Uncoupled Second-Order Vertex Function $\Gamma_{ij}(q^*)$ along with the Inverse Gaussian Correlation Function $S_{ij}^{0-1}(q^*)$ for the Copolymer of MW = 20 000 at Spinodal Temperatures and at Some Selected Compositions

ϕ_1	S_{11}^{0-1}	S_{22}^{0-1}	Γ_{11}	Γ_{22}
0.104	5.337E-01	1.857E-02	248.646	248.441
0.201	1.807E-01	2.122E-02	81.500	81.499
0.301	9.777E-02	2.656E-02	45.349	45.425
0.404	6.338E-02	3.488E-02	33.686	33.817
0.498	4.671E-02	4.612E-02	31.389	31.569
0.598	3.558E-02	6.548E-02	35.145	35.391
0.690	2.860E-02	9.853E-02	47.128	47.463
0.793	2.334E-02	1.873E-01	86.840	87.355
0.899	2.095E-02	6.395E-01	304.358	305.315

^a Pressure is set to 0.1 MPa.

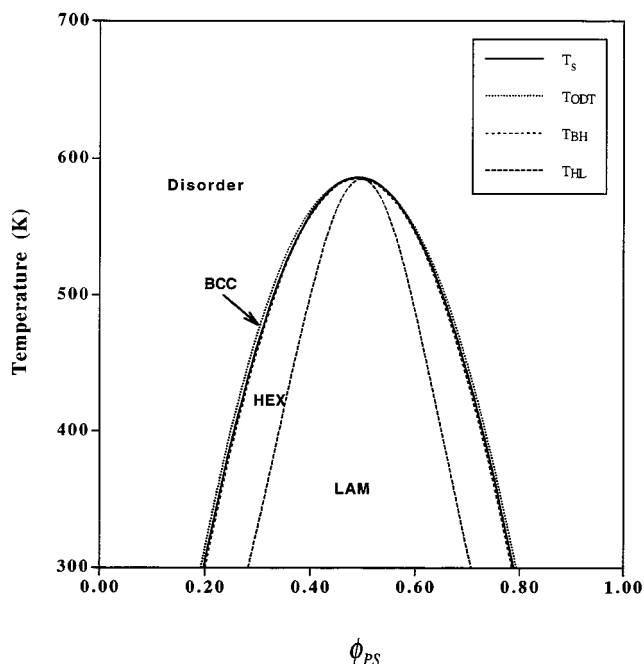


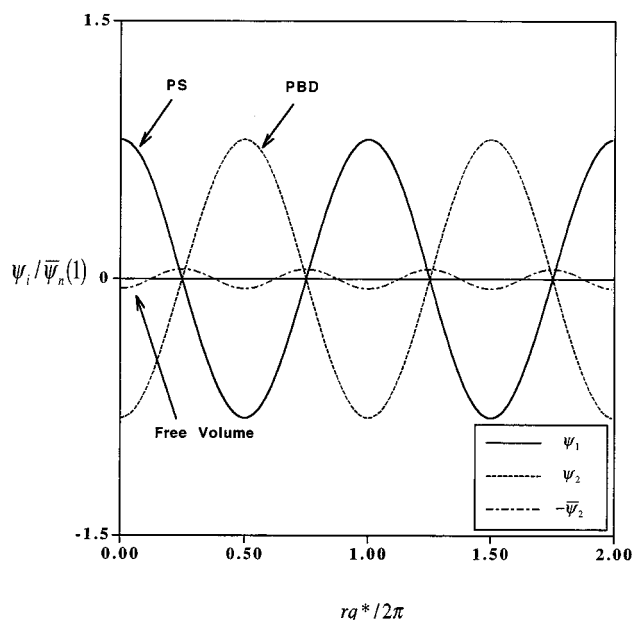
Figure 1. Phase diagram for the P(S-*b*-BD) melt of MW = 20 000. Each line corresponds to a proper transition: T_{ODT} , T_{BH} , and T_{HL} respectively indicate disorder \rightarrow bcc, bcc \rightarrow hex, and hex \rightarrow lam transitions. Spinodals (T_s) are also drawn together. It is seen that the phase diagram is slightly asymmetric around the critical point at $\phi_{PS} = 0.5$.

compressible UCOT systems without compressibility difference between constituents present.

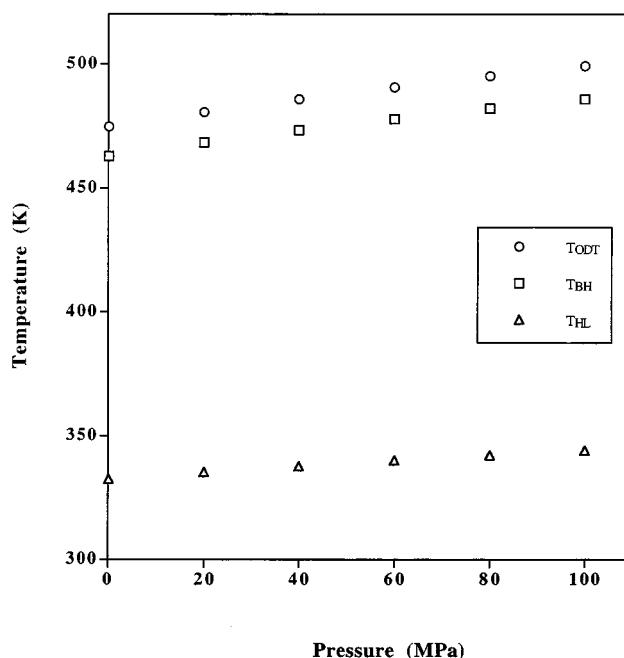
Figure 1 shows spinodals and all the transition temperatures for P(S-*b*-BD) of MW = 20 000 at ambient pressure. As seen in this figure, many features of the present calculation seem similar to those by Leibler.⁵ A general sequence of microphase separation upon cooling (disorder \rightarrow bcc \rightarrow hex \rightarrow lam) is observed for asymmetric copolymers. The spinodal line is enclosed by the disorder \rightarrow bcc transition line. All the transition lines in Figure 1 coincide at the critical point for a symmetric copolymer. However, there are aspects relevant to compressibility. It can be seen that the phase lines are skewed around $\phi_{PS} = 0.5$. The critical composition of $\phi_{PS} = 0.5$ does not offer the threshold of phase lines. The threshold points are slightly shifted to the PBD-side ($\phi_{PS} < 0.5$). For example, the threshold temperature at the disorder \rightarrow bcc transition reads that $T_{thr} = 585.44$ K at $\phi_{PS} = 0.491$. Such minute skewness in the phase diagram originates in the slight difference in the self-interaction parameters $\bar{\epsilon}_{ii}$'s between PS and PBD: $[\bar{\epsilon}_{11} - \bar{\epsilon}_{22}]/\bar{\epsilon}_{11} = 0.01$.

Table 3. Amplitude Parameter $\bar{\psi}_n(i)$ Determined for the Copolymer of MW = 20 000 at the Order–Disorder Transition and at the Indicated Compositions

ϕ_1	$\bar{\psi}_n(1)$	$\bar{\psi}_n(2)$
0.104	2.065E-02	2.411E-07
0.201	3.710E-02	8.671E-07
0.301	4.550E-02	1.422E-06
0.404	3.395E-02	8.258E-07
0.498	1.050E-03	7.948E-10
0.598	3.430E-02	8.336E-07
0.690	4.540E-02	1.405E-06
0.793	3.780E-02	8.882E-07
0.899	2.030E-02	2.288E-07

^a Pressure is set to 0.1 MPa.**Figure 2.** Schematic behavior of the fluctuations in packing densities, $\psi_i(\bar{r})$, for the copolymer of MW = 20 000 at $\phi_{PS} = 0.301$ only along the direction connecting the centers of two dispersed spheres for the bcc morphology at the disorder \rightarrow bcc transition. The fluctuations of free volume fraction, $-\bar{\psi}_2$, are also shown after being magnified substantially. While $\psi_i(\bar{r})$ of each block fluctuates with the wavenumber q^* , the free volume fraction does with the wavenumber $2q^*$ in order to screen the unfavorable cross interactions.

In Table 3, the amplitude $\bar{\psi}_n(i)$ of the order parameter fluctuations obtained at the order–disorder transition and at ambient pressure is tabulated against composition as an illustration for the copolymer of MW = 20 000. Both $\bar{\psi}_n(1)$ and $\bar{\psi}_n(2)$ increase with ϕ_{PS} departing from either PS ($\phi_{PS} = 1$) or PBD ($\phi_{PS} = 0$) homopolymer. As ϕ_{PS} approaches 0.5, both amplitudes reverse their trend to decrease to none, which indicates the critical point. It is seen in this table that $\bar{\psi}_n(2)$ representing the fluctuations of free volume fraction is much smaller than $\bar{\psi}_n(1)$, as expected. Only a slight inhomogeneity of free volume fraction is thus observed. Solving eqs 3 and 4 with respect to ψ_1 and ψ_2 yields $\psi_1 = \eta\bar{\psi}_1 + \phi_{PS}\bar{\psi}_2$ and $\psi_2 = -\eta\bar{\psi}_1 + (1 - \phi_{PS})\bar{\psi}_2$. Therefore, both the ψ_1 and ψ_2 for the density fluctuations of the constituents are mostly determined by $\bar{\psi}_1$. It can also be understood that they fluctuate with the phase angle difference of $\sim 180^\circ$. Figure 2 depicts the plot of the partial view of ψ_i 's for the copolymer at $\phi_{PS} = 0.301$ only along the direction connecting the centers of two dispersed spheres for the bcc morphology. The fluctuations of free volume fraction, $-\bar{\psi}_2$, are also shown in this figure. The excess

**Figure 3.** Various transition temperatures plotted as a function of pressure for the copolymer of MW = 20 000 at $\phi_{PS} = 0.301$. The changes in transition temperatures upon pressurization are shown to be apparently linear up to 100 MPa.

free volume is located at the interface between microphase domains to lower the unfavorable cross-contact energy.

Figure 3 shows the change of transition temperatures upon pressurization for P(S-*b*-BD) of MW = 20 000 at $\phi_{PS} = 0.301$. In this figure, it is observed that not only order–disorder transition temperature, but also subsequent transition temperatures are increased with pressure. Up to 100 MPa, the increase of transition temperatures is quite linear, though there is a hint of systematic downward curvature. This linearity in the order–disorder transition temperature as a function of pressure has been observed by small-angle X-ray scattering experiments on a symmetric P(S-*b*-BD) melt by Stamm and co-workers.^{33,39}

Assuming the apparent linearity of the changes in the transition temperatures, their pressure coefficient, $\Delta T_{tr}/\Delta P$, for the same copolymer as in the previous figures is extracted and plotted in Figure 4. As seen in this figure, $\Delta T_{tr}/\Delta P$ is composition dependent and slightly skewed as the transition temperatures in Figure 1. The threshold composition for $\Delta T_{tr}/\Delta P$ is again shifted, though slightly, to the PBD-side. It is also noted that transitions at higher temperatures are accompanied by higher $\Delta T_{tr}/\Delta P$. The $\Delta T_{tr}/\Delta P$ lines for the indicated transitions are shown to merge at the critical composition of $\phi_{PS} = 0.5$.

To investigate the effect of molecular weights on the transition temperatures and their pressure coefficients, the phase behavior of the same copolymer of MW = 12 400 is calculated. In Figure 5, the order–disorder transition temperatures, T_{odt} , at ambient pressure are plotted as a function of composition and molecular weight. By reducing molecular weight from 20 000 to 12 400, the critical temperature is lowered from 585.2 to 401.8 K. The enhanced mixing for smaller copolymers is caused by the increased combinatorial entropy. The pressure coefficients, $\Delta T_{odt}/\Delta P$ s, of the order–disorder transition temperatures for the two copolymers are

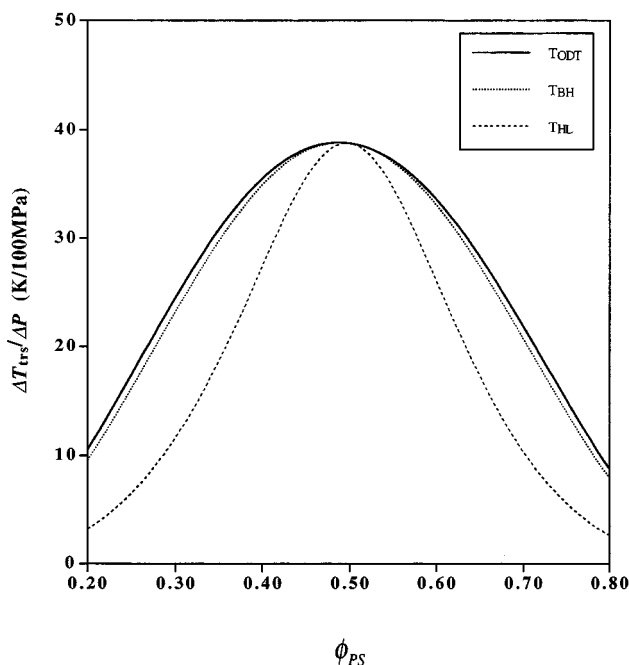


Figure 4. Collection of the pressure coefficients $\Delta T_{\text{trs}}/\Delta P$ of transition temperatures plotted as a function of composition. Each line again corresponds to the indicated transition. All the lines coincide at the critical point.

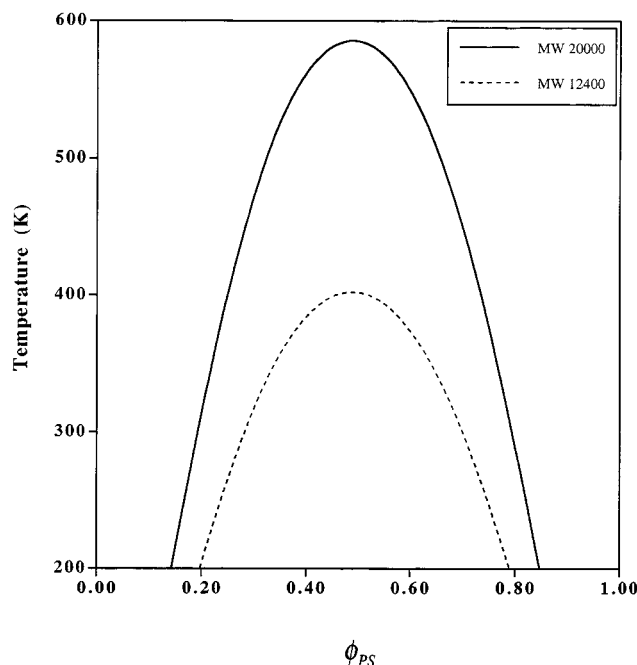


Figure 5. Effect of molecular weight on the order–disorder transition temperatures for the copolymer in the composition range shown. Pressure is fixed at 0.1 MPa.

shown in Figure 6. It is seen that the copolymer of MW = 12 400 possesses diminished $\Delta T_{\text{odt}}/\Delta P$ due to the lowered transition temperatures observed in Figure 5. In the symmetric cases, $\Delta T_{\text{odt}}/\Delta P$ drops from ~ 38 K/100 MPa for the copolymer of higher MW to ~ 17 K/100 MPa for that of lower MW. In the experiments by Stamm and co-workers,³³ a symmetric P(S-*b*-BD) with MW = 14 228 reveals $T_{\text{odt}} = \sim 371$ K and $\Delta T_{\text{odt}}/\Delta P = 20$ K/100 MPa. These experimental results are indeed harmonious with our theoretical calculations considering that concentration fluctuation effects tend to lower T_{odt} .

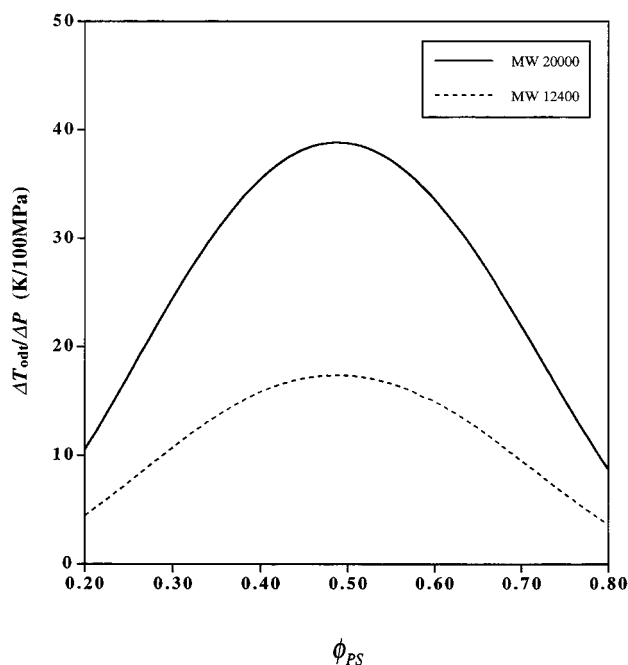


Figure 6. Effect of molecular weight on the pressure coefficients $\Delta T_{\text{odt}}/\Delta P$ of the order–disorder transition temperature for the copolymer in the composition range shown. It is seen that $\Delta T_{\text{odt}}/\Delta P$ is increased with the copolymer molecular weight at the fixed composition.

IV. Relevant Parameters for Phase Behavior

It is our primary interest to elucidate the relevant parameters for phase equilibria calculations. For such purposes, we focus on the quadratic coefficient $\bar{\Gamma}_{11}$ of the Landau free energy in eq 11. As $\bar{\Gamma}_{11}$ is equal to $\eta^2(\Gamma_{11} - 2\Gamma_{12} + \Gamma_{22})$, the $\bar{\Gamma}_{11}$ can be rewritten by putting W_{ij} in Appendix B into Γ_{ij} as

$$\bar{\Gamma}_{11} = \eta^2[S_{11}^{0-1} - 2S_{12}^{0-1} + S_{22}^{0-1}] + \eta \cdot 2\beta[\bar{\epsilon}_{11} - 2\bar{\epsilon}_{12} + \bar{\epsilon}_{22}] \frac{f_p}{2} u(\eta) \quad (12)$$

where f_p is simply 4, and $u(\eta)$, given in eq A2, describes the packing density dependence of the attractive non-bonded interactions. It should be noted that most terms of the complicated W_{ij} are canceled out in $\bar{\Gamma}_{11}$ to yield eq 12. Introducing the dimensionless exchange energy χ as $\chi \equiv \beta[\bar{\epsilon}_{11} + \bar{\epsilon}_{22} - 2\bar{\epsilon}_{12}]$ yields

$$\bar{\Gamma}_{11} = \eta^2[S_{11}^{0-1} - 2S_{12}^{0-1} + S_{22}^{0-1}] - \eta \cdot 2\chi \frac{f_p}{2} |u(\eta)| \quad (13)$$

The $u(\eta)$ is negative at allowable packing densities, so it is replaced with $-|u(\eta)|$. It can be easily seen that the Gaussian terms in the brackets are rewritten as

$$S_{11}^{0-1} - 2S_{12}^{0-1} + S_{22}^{0-1} = \frac{S_{11}^0 + 2S_{12}^0 + S_{22}^0}{\det[S_{ij}^0]} \quad (14)$$

If we denote $\chi f_p/2 \cdot |u(\eta)|$ as χ_{app} , then $\bar{\Gamma}_{11}/\eta$ becomes

$$\frac{\bar{\Gamma}_{11}}{\eta} = \frac{\eta(S_{11}^0 + 2S_{12}^0 + S_{22}^0)}{\det[S_{ij}^0]} - 2\chi_{\text{app}} \quad (15)$$

After the manipulation of all the Gaussian correlation functions,⁴⁰ it can be seen that $\bar{\Gamma}_{11}/\eta$ is indeed identical

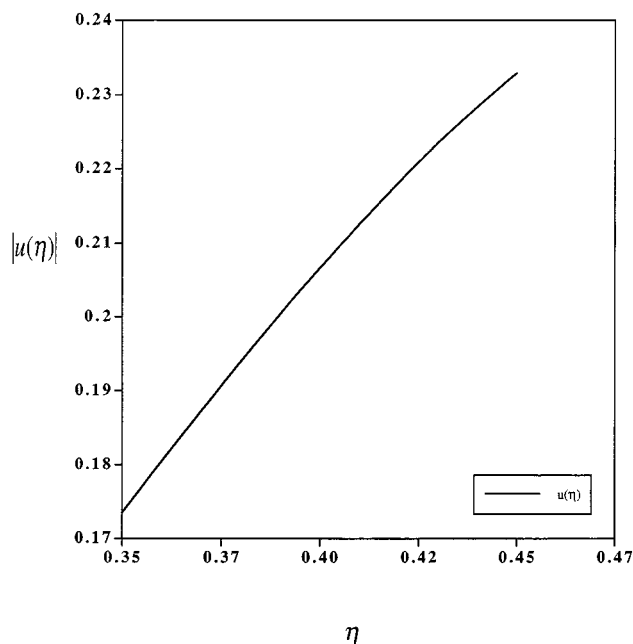


Figure 7. $|u(\eta)|$ plotted as a function of the total packing density η in the useful η range in which either PS or PBD normally lies. It is seen that $|u(\eta)|$ exhibits a fairly linear increase with increasing η .

to the inverse susceptibility in Leibler's theory⁵ except that the only temperature-dependent χ is replaced with a density-dependent χ_{app} . The χ_{app} can be viewed as an apparent Flory–Huggins interaction parameter. This finding demonstrates the close relationship between the present theory and Leibler's. The incompressible limit of the Landau free energy in eq 8 can be formally obtained from setting $\eta = 1$, although the total packing density η cannot exceed 0.74 in the CS model.³¹ In this case, $\bar{\psi}_2$ vanishes and χ_{app} becomes only a function of temperature. As all the vertex functions are evaluated at $\eta = 1$, the Landau free energy by Leibler is retrieved.

The χ for the P(S-*b*-BD) melt is obtained as $\chi = 35.655/T$ from putting all the $\bar{\epsilon}_{ij}$'s into its definition. This χ then gives $T\chi_{app} = 71.310|u(\eta)|$. The $|u(\eta)|$ increases with η in the useful η range shown in Figure 7. We can then state the implicit dependence of $T\chi_{app}$ on temperature, pressure, and composition. The η decreases with T , whereas P does a reverse action to increase η . The ϕ_{PS} dependence of η is slight because $\bar{\epsilon}_{11}$ is larger only by 1% than $\bar{\epsilon}_{22}$. A larger $\bar{\epsilon}_{11}$ renders PS less compressible with a larger η than PBD. Therefore, η is a slightly increasing function of ϕ_{PS} . From the relationship between η and $|u(\eta)|$ in Figure 7, it can be said that $T\chi_{app}$ is an increasing function of ϕ_{PS} and P , but a decreasing function of T .⁴¹

Leibler suggested in his incompressible RPA theory that the only relevant parameters in describing the phase behavior of diblock copolymers are composition and the product (χN) of a chain size and an interaction parameter.⁵ As χ_{app} is identified as an apparent Flory–Huggins parameter, we attempt to collect $r_T\chi_{app}$ at the order–disorder transition for the P(S-*b*-BD) melts of two different molecular weights as a function of composition and pressure in Figure 8. It is clearly shown in this figure that temperature–pressure–MW superposition is constructed for the order–disorder transition temperatures of the copolymer. The same type of plots can be made for the subsequent order–order transitions. It is suggested from this figure, that the only relevant

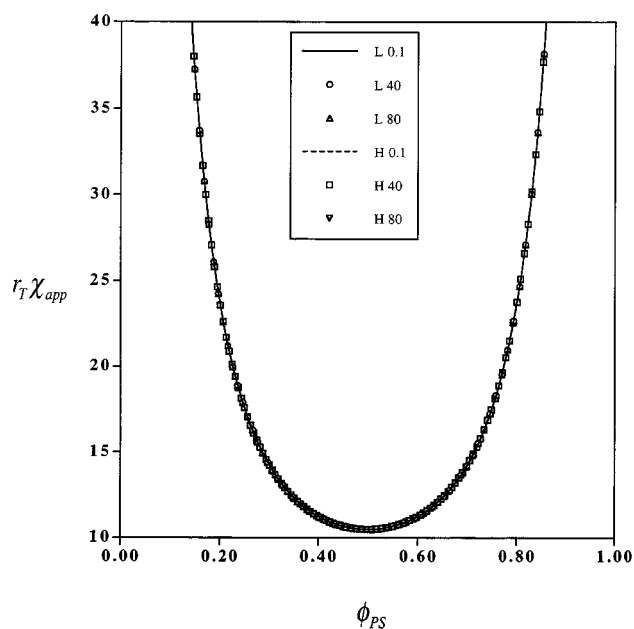


Figure 8. Relevant parameter $r_T\chi_{app}$ ($=r_T\chi_f/2 \cdot |u(\eta)|$) plotted as a function of composition for the P(S-*b*-BD) melts of different molecular weights at the order–disorder transition and at several selected pressures. The L and H indicate the copolymers of MW = 12 400 and 20 000, respectively. The numbers following either L or H represent the applied pressure in MPa. The total packing density η is calculated at the given (T_{odt}, P, ϕ_{PS}) using eq A3. A temperature–pressure–MW superposition is constructed for the order–disorder transition temperatures of the copolymer.

parameters for the compressible P(S-*b*-BD) melts are composition and $r_T\chi_{app}$.

The relevant parameter $r_T\chi_{app}$ can give a unified way to explain all the previous figures. The reduced miscibility upon pressurization,⁴² shown in Figure 3, is caused by the increased contact density of unfavorable interaction pairs by $|u(\eta)|$. The apparent linearity of transition temperatures against pressure in Figure 3 can be explained by the fact that at a fixed composition, $r_T\chi_{app}$ at the corresponding transitions is also fixed. This procedure implies that $\chi|u(\eta)|$ is constant, which in turn yields that transition temperature T_{trs} is proportional to $|u(\eta)|$ or $\Delta T_{trs} \propto \Delta u(\eta)$. The $|u(\eta)|$ is fairly linear with respect to η in the useful range of η . The $\Delta u(\eta)$ is then roughly proportional to $\Delta\eta$. From the definition of the isothermal compressibility β_T ($\equiv 1/\eta \partial\eta/\partial P$), it can be shown that $\Delta\eta = \eta_0\beta_T(P - P_0) + O(|\beta_T(P - P_0)|^2)$, where η_0 is the packing density at a reference pressure P_0 . It can then be said that $\Delta\eta$ is roughly proportional to ΔP ($=P - P_0$) as β_T is usually low for polymers. Summarizing all yields a conclusion that ΔT_{trs} is largely proportional to ΔP , as shown in Figure 3.

It is seen in Figure 4 that the pressure coefficient $\Delta T_{trs}/\Delta P$ of various transition temperatures exhibits the composition dependence in a fashion similar to the transition temperatures themselves shown in Figure 1. This result can also be explained in terms of χ_{app} . In Figure 1, the transition temperatures increase as ϕ_{PS} approaches the threshold composition near $\phi_{PS} = 0.5$. The packing density η or the function $|u(\eta)|$ decreases accordingly. The copolymer then becomes more compressible. Therefore, there is more room to experience the increase in the density of unfavorable contacts upon pressurization, which eventually leads to the increase in $\Delta T_{trs}/\Delta P$. The magnitude of $\Delta T_{trs}/\Delta P$ for various

transitions at a fixed composition increases from lam \rightarrow hex to hex \rightarrow bcc, and then to bcc \rightarrow disorder transition because of the increased compressibility in that order. At the critical point, all the transition temperatures coincide, which results in the observed coincidence of $\Delta T_{\text{trs}}/\Delta P$.

The pressure coefficient $\Delta T_{\text{odt}}/\Delta P$ of the order-disorder transition at a fixed composition turns out to be increased with the molecular weight, as seen in Figure 6. Such a result is again caused by the fact that the copolymer of higher molecular weight generally exhibits higher transition temperatures than that of lower molecular weight, as shown in Figure 5. The heavier copolymer at the transition temperatures becomes more compressible and thus possesses larger $\Delta T_{\text{odt}}/\Delta P$ than the lighter one. It is notable in Figures 5 and 6 that if copolymers with different molecular weights exhibit the same transition temperatures, they possess the same pressure dependence of transition temperatures. For example, the copolymer of MW = 12 400 at $\phi_{\text{PS}} = \sim 0.5$ and that of MW = 20 000 at $\phi_{\text{PS}} = \sim 0.25$ reveal near identical T_{odt} 's and indeed $\Delta T_{\text{odt}}/\Delta P$'s. This result again demonstrates the usefulness of the extracted relevant parameter $r\chi_{\text{app}}$ to describe the compressibility effects on microphase separation in UCOT systems.

V. Summary

A mean-field Landau free energy for a compressible UCOT diblock copolymer has been formulated. Both the constituent polymers comprising the block copolymer are assumed to have no compressibility difference between them as the simplest but the most important case. The UCOT behavior is driven by unfavorable interactions between constituents. The microphase segregating copolymer system experiences the inhomogeneity not only of packing density of each constituent, but also of free volume fraction. Excess free volume has been shown to be present at the interface between microphase domains to screen such unfavorable energetics. The well-known sequence of microphase separation transition, i.e., disorder \rightarrow bcc \rightarrow hex \rightarrow lam, upon cooling is observed as in the incompressible situation. A critical point is existent for a symmetric copolymer in the present case with no compressibility difference between constituents.

It has been revealed that the only relevant parameters in describing phase behavior are composition and the product $r\chi_{\text{app}}$ ($=r\chi f_p/2 \cdot |u(\eta)|$), which is dependent on system compressibility. The elicited relevant parameter $r\chi_{\text{app}}$ has yielded the following predictions:

(1) A transition temperature at a fixed composition exhibits largely a linear increase upon pressurization owing to the constancy of $\chi|u(\eta)|$ at the transition.

(2) The pressure coefficients of transition temperatures at a fixed composition increase from lam \rightarrow hex to hex \rightarrow bcc and then to bcc \rightarrow disorder transitions because of the increased compressibility with the transition temperatures. Such coefficients coincide at the critical point.

(3) The pressure coefficients of transition temperatures at a fixed composition increase with the molecular weights because heavier copolymers exhibit higher transition temperatures and thus increased compressibility than lighter ones.

The present Landau analysis has been successfully applied to the P(S-*b*-BD) melt, which is our model

system here. The obtained theoretical predictions, though based on the assumption of suppressed compressibility difference between constituents, are considered to be applicable to many other UCOT systems including another widely studied diblock copolymer of PS and polyisoprene.⁴³

Acknowledgment. This work has been supported by Korea Science and Engineering Foundation through Hyperstructured Organic Materials Research Center (HOMRC).

Appendix A. Cho-Sanchez Equation-of-State Model

Let us consider a binary blend system of two polymers with N_1 chains of r_1 -mers and N_2 chains of r_2 -mers in a fixed volume. Each polymer chain is simplified to be the linear chain of tangent spheres or monomers, and all monomers in the system are assumed to have the identical diameter σ .

The Cho-Sanchez (CS) equation-of-state model^{31,27} for polymer blends suggests the free energy as $A = A_0^{\text{id}} + A_0^{\text{EV}} + U^{\text{nb}}$. The A_0^{id} and A_0^{EV} respectively represent the ideal free energy of the noninteracting Gaussian blend system and the contribution to the free energy from the excluded volume effects. The U^{nb} stands for the attractive interactions between nonbonded monomers. Each term of the free energy is written explicitly in the following analytical equation

$$\frac{\beta A}{rN} = \sum \frac{\phi_i}{r_i} \ln \frac{6\eta \phi_i I_i \Lambda_i^{3r_i}}{\pi r_i \rho^3 z_i e} + \left\{ \frac{3}{2} \left[\frac{1}{(1-\eta)^2} - \left(1 - \frac{1}{r} \right) \frac{1}{1-\eta} \right] - \frac{1}{r} \left[\ln(1-\eta) + \frac{3}{2} \right] \right\} + \frac{f_p}{2} \bar{\epsilon} u(\eta) \quad (\text{A1})$$

where $N = N_1 + N_2$ is the total number of chains and $r = (r_1 N_1 + r_2 N_2)/N$ denotes the average chain size. The ϕ_i is the close-packed volume fraction of i -monomers, and thus $\phi_i = r_i N_i / rN$. I_i and Λ_i imply the symmetry number of i -chains and the thermal de Broglie wavelength of monomers on i -chains, respectively. The symbol z_i implies the conformational partition function of Gaussian i -chains, which will be left as an unspecified constant here. The η denotes the total packing density that implies the fraction of volume occupied by all the chains. The symbol e indicates the transcendental number of 2.718 and β is $1/kT$ as usual.

The $u(\eta)$ in eq 1 describes the packing density dependence of attractive nonbonded interactions as

$$u(\eta) = [(\gamma/C)^{p/3} \eta^{p/3} - (\gamma/C)^2 \eta^2] \quad (\text{A2})$$

where $\gamma = 1/\sqrt{2}$, $C = \pi/6$, and $p = 12$. This functional form for $u(\eta)$ originates in the Lennard-Jones (L-J) potential acting between two monomers. The f_p in eq A1 is a numeric prefactor associated with the L-J potential, and simply $f_p = 4$. The parameter $\bar{\epsilon}$, defined as $\bar{\epsilon} = \sum_{ij} \phi_i \phi_j \bar{\epsilon}_{ij}$, describes the characteristic energy of the blend, where $\bar{\epsilon}_{ij}$ implies the L-J potential depth of the attractive interactions between two monomers on i - and j -chains.

To apply the free energy in eq A1 to a specific blend system, one requires various molecular parameters such as $\bar{\epsilon}_{ij}$, r_i , and σ for given homopolymers and $\bar{\epsilon}_{ij}$ for cross interactions between different homopolymers. Homopolymer parameters can be obtained from fitting measured

volumetric data to the following equation of state:

$$\beta P = \frac{1}{v^*} \left[\frac{3}{2} \frac{(\eta^2 + \eta^3)}{(1 - \eta)^3} + \frac{\eta}{r} \frac{(1 + \eta/2)}{(1 - \eta)^2} \right] + \frac{f_p}{2} \frac{\beta \bar{\epsilon}}{v^*} \eta^2 \frac{\partial u(\eta)}{\partial \eta} \quad (\text{A3})$$

where v^* ($= \pi\sigma^3/6$) is the volume of one monomer. Equation A3 results from the differentiation of eq A1 with respect to volume. The cross-interaction parameter $\bar{\epsilon}_{ij}$ is commonly estimated as $\bar{\epsilon}_{ij} = \xi(\bar{\epsilon}_i \bar{\epsilon}_j)^{1/2}$ with an adjustable parameter ξ , which can be determined from various mixture behavior such as the heat of mixing, spinodals, and binodals.

Appendix B. Compressible RPA

Recently, the present author developed a compressible RPA theory to calculate the second-order monomer–monomer correlation function $G_{ij}^{(2)}$, or equivalently S_{ij} , and higher-order correlation functions $G^{(n)}$'s for the analysis of phase segregation in compressible polymer blends and block copolymers.^{27,28} The theory was formulated from combining Akcasu et al.'s general compressible RPA formalism^{29,30} with the CS model. The basic idea of the theory follows the spirit of the incompressible RPA by Leibler.⁵ The Landau expansion of the free energy is expressed as a series in a hypothetical external potential U_i , which is conjugate to the order parameter ψ_i . The ψ_i can also be expanded as a series in U_i . The coefficients appearing in the series for ψ_i are the correlation functions $G^{(n)}$'s. In estimating ψ_i , the correlation functions $G^{(n)}$ are supposed to be equal to those of noninteracting Gaussian copolymer chains, which are denoted as $G^{(n)0}$. The external potential U_i is then substituted with U_i^{eff} , which is corrected as $U_i^{\text{eff}} = U_i + W_{ij}\psi_j$ to properly take the interaction effects into account by an interaction field W_{ij} . W_{ij} replaces the simple Flory–Huggins χ to account for the desired compressibility effects and is formulated from the CS model. The resultant self-consistent field equation is solved in an iterative technique to obtain correlation functions.²⁸ The correlation functions then yield the vertex functions as

$$\Gamma_{ij}^{(2)} = S_{ij}^{-1} = S_{ij}^{0-1} + \beta W_{ij} \quad (\text{B1})$$

$$\Gamma_{ijk}^{(3)}(\bar{q}_1, \bar{q}_2, \bar{q}_3) = -S_{pi}^{0-1}(\bar{q}_1) G_{plm}^{(3)0}(\bar{q}_1, \bar{q}_2, \bar{q}_3) S_{lj}^{0-1}(\bar{q}_2) S_{mk}^{0-1}(\bar{q}_3) \quad (\text{B2})$$

$$\begin{aligned} \Gamma_{abcd}^{(4)}(\bar{q}_1, \bar{q}_2, \bar{q}_3, \bar{q}_4) = & \int d\bar{q} S_{ko}^{0-1}(\bar{q}) \{ G_{ijk}^{(3)0}(\bar{q}_1, \bar{q}_2, \bar{q}) G_{opr}^{(3)0}(-\bar{q}, \bar{q}_3, \bar{q}_4) + \\ & G_{ipk}^{(3)0}(\bar{q}_1, \bar{q}_3, \bar{q}) G_{ojr}^{(3)0}(-\bar{q}, \bar{q}_2, \bar{q}_4) + \\ & G_{irk}^{(3)0}(\bar{q}_1, \bar{q}_4, \bar{q}) G_{ojp}^{(3)0}(-\bar{q}, \bar{q}_2, \bar{q}_3) \} - \\ & G_{ijpr}^{(4)0}(\bar{q}_1, \bar{q}_2, \bar{q}_3, \bar{q}_4) S_{ia}^{0-1}(\bar{q}_1) S_{jb}^{0-1}(\bar{q}_2) S_{pc}^{0-1}(\bar{q}_3) S_{rd}^{0-1}(\bar{q}_4) \end{aligned} \quad (\text{B3})$$

It should be kept in mind that the vertex functions $\Gamma^{(n)}$ ($\bar{q}_1, \dots, \bar{q}_n$) are nonvanishing only if $\sum_{i=1}^n \bar{q}_i$ vanishes.

$$[\bar{\Gamma}_{ij}^{(2)}] = \begin{bmatrix} \eta^2(\Gamma_{11}^{(2)} - 2\Gamma_{12}^{(2)} + \Gamma_{22}^{(2)}) \\ \eta\phi_1(\Gamma_{11}^{(2)} - \Gamma_{12}^{(2)}) + \eta(1 - \phi_1)(\Gamma_{12}^{(2)} - \Gamma_{22}^{(2)}) \end{bmatrix} \quad (\text{C4})$$

All the Gaussian correlation functions used here can be obtained from a slight modification of those in Appendices B and C of ref 5. Those Gaussian functions in ref 5 are to be multiplied by the total packing density η , which indicates the diluted contact probability owing to free volume.

The interaction field W_{ij} is obtained from the nonideal free energy, $A_0^{\text{EV}} + U^{\text{nb}}$, of the CS model. The W_{ij} then consists of the two terms L_{ij} and $\epsilon_{ij}^{\text{app}}$, which are formulated from A_0^{EV} and U^{nb} , respectively

$$\beta W_{ij} = L_{ij}(\eta) - \beta \epsilon_{ij}^{\text{app}}(\eta) \quad (\text{B4})$$

where L_{ij} and $\epsilon_{ij}^{\text{app}}$ are given as

$$\begin{aligned} L_{ij}(\eta) = & \frac{3}{2} \left[\frac{4}{(1 - \eta)^3} + \frac{6\eta}{(1 - \eta)^4} - \right. \\ & \left. \left(2 - \frac{1}{r_i} - \frac{1}{r_j} \right) \frac{1}{(1 - \eta)^2} - \left(\eta - \frac{\eta}{r} \right) \frac{2}{(1 - \eta)^3} \right] + \\ & \left(\frac{1}{r_i} + \frac{1}{r_j} \right) \frac{1}{1 - \eta} + \frac{\eta}{r} \frac{1}{(1 - \eta)^2} \end{aligned} \quad (\text{B5})$$

and

$$\begin{aligned} -\beta \epsilon_{ij}^{\text{app}}(\eta) = & \beta \bar{\epsilon}_{ij} f_p \frac{u(\eta)}{\eta} + \beta \left(\sum_k \eta_k \{ \bar{\epsilon}_{ik} + \bar{\epsilon}_{jk} \} \right) f_p \frac{\partial}{\partial \eta} \left(\frac{u(\eta)}{\eta} \right) + \\ & \frac{1}{2} \beta \left(\sum_{kl} \eta_k \eta_l \bar{\epsilon}_{kl} \right) f_p \frac{\partial^2}{\partial \eta^2} \left(\frac{u(\eta)}{\eta} \right) \end{aligned} \quad (\text{B6})$$

The interaction field W_{ij} given above was first derived for polymer blends with the close-packed volume fraction ϕ_i of i -monomers. The W_{ij} for polymer blends is then adopted for the corresponding block copolymers with the same ϕ_i .^{27,28}

Appendix C. Vertex Functions upon Change in the Order Parameters

The order parameter ψ_i in eq 1 is converted to a new order parameter $\bar{\psi}_i$ in eqs 3 and 4 by the following tensor equation

$$\bar{\psi}_i = M_{ij} \psi_j \quad (\text{C1})$$

where M_{ij} is defined as

$$[M_{ij}] = \begin{bmatrix} \frac{1}{\eta}(1 - \phi_1) & -\frac{\phi_1}{\eta} \\ 1 & 1 \end{bmatrix} \quad (\text{C2})$$

The vertex functions $\Gamma^{(n)}$ in the Landau expansion of the free energy in eq 2 is then replaced with the proper vertex function $\bar{\Gamma}^{(n)}$ as

$$\bar{\Gamma}_{i_1 \dots i_n}^{(n)} = \Gamma_{j_1 \dots j_n}^{(n)} M_{j_1 i_1}^{-1} \dots M_{j_n i_n}^{-1} \quad (\text{C3})$$

After some mathematical manipulation of eq C3, the first three vertex functions $\bar{\Gamma}^{(n)}$'s can be given as

$$\Gamma_{ijk}^{(3)}(\bar{q}_1, \bar{q}_2, \bar{q}_3) = -V_{mi}(\bar{q}_1)G_{mno}^{(3)0}(\bar{q}_1, \bar{q}_2, \bar{q}_3)V_{nj}(\bar{q}_2)V_{ok}(\bar{q}_3) \quad (C5)$$

$$\begin{aligned} \bar{\Gamma}_{abcd}^{(4)}(\bar{q}_1, \bar{q}_2, \bar{q}_3, \bar{q}_4) = & \int d\bar{q} S_{ko}^{-1}(\bar{q}) \{ G_{ijk}^{(3)0}(\bar{q}_1, \bar{q}_2, \bar{q}) G_{opr}^{(3)0}(-\bar{q}, \bar{q}_3, \bar{q}_4) + \\ & G_{ipk}^{(3)0}(\bar{q}_1, \bar{q}_3, \bar{q}) G_{ojr}^{(3)0}(-\bar{q}, \bar{q}_2, \bar{q}_4) + \\ & G_{irk}^{(3)0}(\bar{q}_1, \bar{q}_4, \bar{q}) G_{ojp}^{(3)0}(-\bar{q}, \bar{q}_2, \bar{q}_3) \} - \\ & G_{ijpr}^{(4)0}(\bar{q}_1, \bar{q}_2, \bar{q}_3, \bar{q}_4) V_{ia}(\bar{q}_1) V_{jb}(\bar{q}_2) V_{pc}(\bar{q}_3) V_{rd}(\bar{q}_4) \quad (C6) \end{aligned}$$

where a new tensor V_{ij} in eqs C5 and C6 is defined as the combination of S_{ij}^{0-1} and M_{ij} as

$$[V_{ij}] \equiv [S_{ik}^{0-1} M_{kj}^{-1}] = \begin{bmatrix} \eta(S_{11}^{0-1} - S_{12}^{0-1}) & \phi_1 S_{11}^{0-1} + (1 - \phi_1) S_{12}^{0-1} \\ \eta(S_{21}^{0-1} - S_{22}^{0-1}) & \phi_1 S_{21}^{0-1} + (1 - \phi_1) S_{22}^{0-1} \end{bmatrix} \quad (C7)$$

It should be noted that V_{il} in eq C7 is independent of η because S_{ij}^{0-1} is proportional to $1/\eta$. The V_{il} is indeed frequently employed to obtain higher-order vertex functions Γ_3 and Γ_4 in the incompressible RPA by Leibler.⁵

Among various $\bar{\Gamma}^{(n)}$ s, $\bar{\Gamma}_{111}^{(3)}$ and $\bar{\Gamma}_{111}^{(4)}$ are of our special interest. As seen in eqs C5 and C6, only V_{il} is used to calculate those two vertex functions. It can then be easily seen that $\bar{\Gamma}_{111}^{(3)}$ and $\bar{\Gamma}_{111}^{(4)}$ become identical with $\eta\Gamma_3$ and $\eta\Gamma_4$, i.e., the product of the packing density η and Leibler's vertex functions Γ_3 and Γ_4 , respectively.

References and Notes

- (1) Aggarwal, S. L. *Block Copolymers*; Plenum Press: New York, 1970.
- (2) *Developments in Block Copolymers-I*; Goodman, I., Ed.; Applied Science Publishers: New York, 1982.
- (3) *Thermoplastic Elastomers*; Holden, G., Legge, N. R., Quirk, R. P., Schroeder, H. E., Eds.; Hanser: New York, 1996.
- (4) Hamley, I. W. *The Physics of Block Copolymers*; Oxford University Press: New York, 1998.
- (5) Leibler, L. *Macromolecules* **1980**, *13*, 1602.
- (6) Fredrickson, G. H.; Helfand, E. *J. Chem. Phys.* **1987**, *87*, 697.
- (7) Milner, S. T.; Olmsted, P. D. *J. Phys. II* **1997**, *7*, 249.
- (8) Hamley, I. W.; Bates, F. J. *Chem. Phys.* **1994**, *100*, 6813.
- (9) Podnaks, V. E.; Hamley, I. W. *JETP Lett.* **1996**, *64*, 617.
- (10) Podnaks, V. E.; Hamley, I. W. *Pisma Zh. Eksp. Teor. Fiz.* **1996**, *64*, 564.
- (11) Hamley, I. W.; Podnaks, V. E. *Macromolecules* **1997**, *30*, 3701.
- (12) Russell, T. P.; Karis, T. E.; Gallot, Y.; Mayes, A. M. *Nature* **1994**, *368*, 729.
- (13) Karis, T. E.; Russell, T. P.; Gallot, Y.; Mayes, A. M. *Macromolecules* **1995**, *28*, 1129.
- (14) Ruzette, A.-V. G.; Banerjee, P.; Mayes, A. M.; Pollard, M.; Russell, T. P.; Jerome, R.; Slawacki, T.; Hjelm, R.; Thiyagarajan, P. *Macromolecules* **1998**, *31*, 8509.
- (15) Mansky, P.; Tsui, O. K. C.; Russell, T. P.; Gallot, Y. *Macromolecules* **1999**, *32*, 4832.
- (16) McMullen, W. E.; Freed, K. F. *Macromolecules* **1990**, *23*, 255.
- (17) Dudowicz, J.; Freed, K. F. *Macromolecules* **1990**, *23*, 1519.

- (18) Tang, H.; Freed, K. F. *Macromolecules* **1991**, *24*, 958.
- (19) Tang, H.; Freed, K. F. *J. Chem. Phys.* **1991**, *94*, 1572.
- (20) Dudowicz, J.; Freed, K. F. *J. Chem. Phys.* **1992**, *96*, 9147.
- (21) Freed, K. F.; Dudowicz, J. *J. Chem. Phys.* **1992**, *97*, 2105.
- (22) Dudowicz, J.; Freed, K. F. *Macromolecules* **1993**, *26*, 213.
- (23) Dudowicz, J.; Freed, K. F. *Macromolecules* **1995**, *28*, 6625.
- (24) Yeung, C.; Desai, R. C.; Shi, A. C.; Noolandi, J. *Phys. Rev. Lett.* **1994**, *72*, 1834.
- (25) Bidkar, U. R.; Sanchez, I. C. *Macromolecules* **1995**, *28*, 3963.
- (26) Hino, T.; Prausnitz, J. M. *Macromolecules* **1998**, *31*, 2636.
- (27) Cho, J. *Macromolecules* **2000**, *33*, 2228.
- (28) Cho, J. *Macromolecules* **2001**, *34*, 1001.
- (29) Akcasu, A. Z.; Tombakoglu, M. *Macromolecules* **1990**, *23*, 607.
- (30) Akcasu, A. Z.; Klein, R.; Hammouda, B. *Macromolecules* **1993**, *22*, 1238.
- (31) Cho, J.; Sanchez, I. C. *Macromolecules* **1998**, *31*, 6650.
- (32) This simple picture of free volume inhomogeneity relies on the assumption that compressibility difference between constituents is absent or not important in the practical sense.
- (33) Ladynski, H.; Odorico, D.; Stamm, M. *J. Non-Cryst. Solids* **1998**, *235-237*, 491.
- (34) This choice of order parameters follows the incompressible RPA treatment for diblock copolymer chains in a neutral solvent by Fredrickson and Leibler. One can put $\phi_1 = 0.5$ into eq 3 for further simplification. See: Fredrickson, G. H.; Leibler, L. *Macromolecules* **1989**, *22*, 1238.
- (35) Quach, A.; Simha, R. *J. Appl. Phys.* **1971**, *42*, 4592.
- (36) Barlow, J. W. *Polym. Eng. Sci.* **1978**, *18*, 238.
- (37) It is assumed for the simplification of the present theory that all the monomers in the system have an identical diameter σ .
- (38) Such unfavorable energetics in the PS/PBD system yields a positive volume change Δv upon mixing. For example, PS and PBD, both being of MW = 10000, experience $\Delta v/v = 4.916 \times 10^{-4}$ at $T = 500$ K when $\phi_{PS} = 0.5$.
- (39) It was also found that the spinodal point for the symmetric diblock copolymer of MW = ~ 15 700 from PS and deuterated PBD was increased by ~ 12 K upon pressurization up to 200 MPa. However, the order-disorder transition for this system did not show apparent changes with pressure. See: Frielinghaus, H.; Abbas, B.; Schwahn, D.; Willner, L. *Europhys. Lett.* **1998**, *44* (5), 606.
- (40) It should be noted that the Gaussian correlation function S_{ij}^0 is proportional to η owing to free volume.
- (41) The $T_{\chi_{F-H}}$, where χ_{F-H} is the Flory-Huggins interaction parameter obtained from the analysis of the phase behavior of the PS/PBD mixture, is often expressed empirically as $T_{\chi_{F-H}} = A + B\phi_{PS} - CT$ or simply $T_{\chi_{F-H}} = A - CT$ with positive constants A , B , and C . This result is indeed harmonious with the behavior of the theoretical $T_{\chi_{app}}$.
- (42) While this phenomenon is observed for the P(S-*b*-BD) melt and others, Frielinghaus et al. reported that the diblock copolymer of polyethylene and poly(ethylene-propylene), denoted as P(EE-*b*-EP), of MW = 76 000 at $\phi_{PEP} = 0.65$ reveals the reverse trend: $\Delta T_{odt}/\Delta P \approx -17$ K/100 MPa at the order-disorder transition. In the case of the P(EE-*b*-EP) melt, compressibility difference between blocks is considered to affect transition temperatures. The exertion of pressure reduces compressibility difference, which in general enhances miscibility. As mentioned in the main text, the increased contact density of unfavorable pair interactions upon pressurization does the reverse action. Those two competing effects are considered to cause in this case the retreat of phase line. See: Frielinghaus, H.; Schwahn, D.; Mortensen, K.; Almdal, K.; Springer, T. *Macromolecules* **1996**, *29*, 3263.
- (43) Hajduk, D. A.; Gruner, S. M.; Erramilli, S.; Register, R. A.; Fetters, L. J. *Macromolecules* **1996**, *29*, 1473.

MA0100910